

parameters and more computations, and its use does not always result in significantly better restorations. A geometrical PSF which has approximately the same first spectral null as the physical PSF can be used without significant loss in the visual quality of the restoration when the SNR is at or below 30 dB. Aliasing in the discrete representation of the physical PSF can be minimized by utilizing a high frequency PSF representation, which may be used to obtain improved restorations when the SNR is very high (>40 dB).

REFERENCES

- [1] M. I. Sezan, G. Pavlovic, A. M. Tekalp, and A. T. Erdem, "On modeling the focus blur in image restoration," in *Proc. IEEE Int. Conf. Acoust., Speech, and Signal Proc.*, pp. 2485–2488, Toronto, Canada, May 1991.
- [2] A. E. Savakis and H. J. Trussell, "Restorations of real defocused images using blur models based on geometrical and diffraction optics," in *Proc. IEEE Southeastcon 1991*, Williamsburg, VA, Apr. 1991.
- [3] A. E. Savakis and H. J. Trussell, "Sampling and SNR considerations for optical blur models," in *Proc. 1991 Conf. in Sciences and Systems*, Baltimore, MD, Mar. 1991.
- [4] H. C. Lee, "Review of image-blur models in a photographic system using the principles of optics," *Opt. Eng.*, vol. 29, pp. 405–421, May 1990.
- [5] P. A. Stokseth, "Properties of a defocused optical system," *J. Opt. Soc. Amer.*, vol. 59, pp. 1314–1321, Oct. 1969.
- [6] D. B. Gennery, "Determination of optical transfer function by inspection of frequency-domain plot," *J. Opt. Soc. Amer.*, vol. 63, pp. 1571–1577, Dec. 1973.
- [7] M. M. Chang, A. M. Tekalp, and A. T. Erdem, "Blur identification using the bispectrum," *IEEE Trans. Acoust., Speech, Signal Processing*, vol. 39, pp. 2323–2325, Oct. 1991.
- [8] H. J. Trussell and A. E. Savakis, "Blur identification by statistical analysis," in *Proc. 1991 Int. Conf. Acoust., Speech, and Signal Proc.*, pp. 2493–2496, Toronto, Canada, May 1991.

Color Edge Detection Using Vector Order Statistics

P. E. Trahanias and A. N. Venetsanopoulos

Abstract—Color edge detection based on vector order statistics is proposed in this work. In this approach, a color image is treated as a vector field and the edge information carried directly by the vectors is exploited. A class of color edge detectors is defined as the minimum over the magnitudes of linear combinations of the sorted vector samples. From this class, a specific edge detector is obtained and its performance characteristics are studied. A quantitative evaluation and comparison to other color edge detectors, using Pratt's figure of merit and an artificially generated test image, shows results which favor our approach. Moreover, edge detection results obtained from real color images demonstrate the efficiency of the proposed color edge detector.

I. INTRODUCTION

Traditionally, color edge detection has been treated as an extension of the monochrome edge detectors to color images. The use of the Hueckel edge operator in the luminance, chrominance color space has been proposed in [1] and the application of compass

Manuscript received January 14, 1992; revised August 2, 1992. The associate editor coordinating the review of this paper and approving it for publication was Prof. Roland T. Chin.

The authors are with the Department of Electrical and Computer Engineering, University of Toronto, Toronto, Ontario, Canada M5S 1A4.
IEEE Log Number 9206912.

gradient edge detectors to color images has been studied in [2]. The gradient operators proposed for gray-level images can be extended to color images by taking the vector sum of the gradients of the individual components [3], [4]. However, this approach may be very unsatisfactory in certain cases where the image gradients show the same strength but in opposite directions [4]. Then, the vector sum of the gradients would provide a null gradient. Consequently, it is desirable to approach the problem of color edge detection in the vector space. This has been studied recently by using vector gradient operators [4], [5]. In these approaches, color images are treated as vector fields, as has initially been suggested in [6]. In another approach, reported in [3], the entropy operator is employed as an edge detector for monochrome as well as for color images.

A different approach to the problem of color edge detection is proposed in this work, which is based on vector order statistics [7]. This approach resembles the morphological edge detectors for monochrome images [8]. These detectors essentially operate by detecting local minima and maxima in the image function and combining them in a suitable way in order to produce a positive response for an edge pixel. Since there is no exact equivalent of the min-max scalar operators for multivariate (vector) variables, we rely on the vector ordering schemes that have been proposed in the statistics literature [7]. Based on the R-ordering scheme [7], a class of color edge detectors is defined using the magnitudes of linear combinations of the sorted vector samples. More specifically, it is defined as the minimum over these magnitudes. Different coefficients in the linear combinations result in different edge detectors that vary in simplicity and in efficiency. A set of coefficients is selected that results in a robust design, as it is experimentally verified.

In what follows, a brief introduction to vector order statistics is first given and then our approach to color edge detection is described. Finally, evaluation results as well as edge detection results obtained from real images are presented.

II. VECTOR ORDER STATISTICS

Ordering of multivariate data can not be uniquely defined. There has been a number of ways proposed to perform multivariate data ordering that are generally classified into [7]: marginal ordering (M-ordering), reduced or aggregate ordering (R-ordering), partial ordering (P-ordering), and conditional ordering (C-ordering). R-ordering is employed in this work and is further explained in the sequel. This ordering scheme is adopted since it gives a natural definition of the *vector median* as the first sample in the sorted vectors, and large values of the aggregate distance give an accurate description of the *vector outliers*. Moreover, the other ordering schemes suffer from certain drawbacks in the case of color image processing. M-ordering corresponds actually to a componentwise processing and P-ordering implies the construction of convex hulls which is very difficult in 3-D's. C-ordering is simply an ordering according to a specific component and it does not utilize the information content of the other signal components. The reader interested in vector ordering schemes is referred to [7] for a thorough discussion of the subject.

Let \mathbf{X} represent a p -dimensional multivariate $\mathbf{X} = [X_1, X_2, \dots, X_p]^T$ where X_l , $l = 1, 2, \dots, p$ are random variables and let \mathbf{X}^i , $i = 1, 2, \dots, n$ be an observation of \mathbf{X} . Each \mathbf{X}^i is a p -dimensional vector $\mathbf{X}^i = [X_1^i, X_2^i, \dots, X_p^i]^T$. In R-ordering, each multivariate observation is reduced to a scalar value d_i according to a distance criterion. If we employ as a distance metric the aggregate

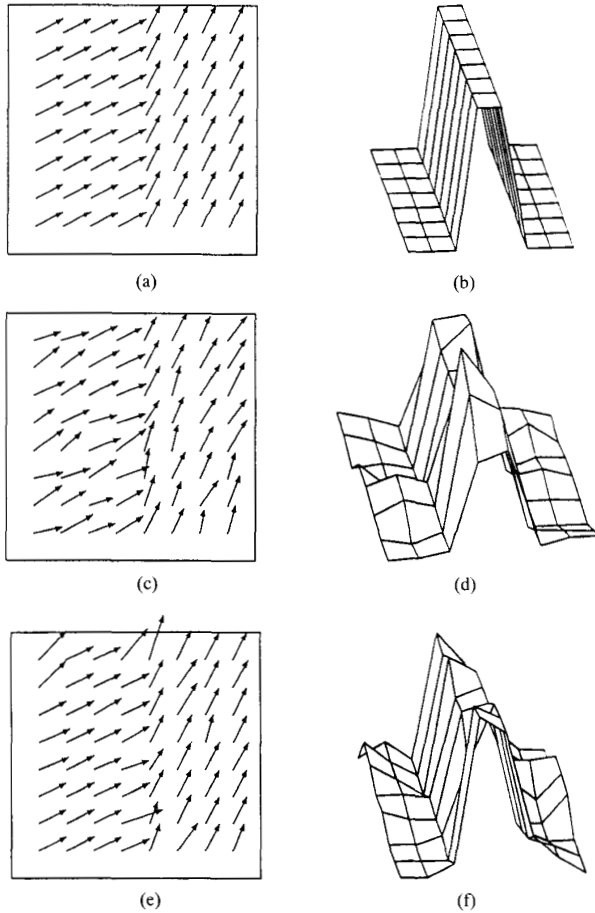


Fig. 1. Response of MVD to noise contaminated edge. (a) Initial edge, (b) Response of MVD to (a), (c) edge (a) corrupted with gaussian noise, (d) response of MVD to (c), (e) edge (a) corrupted with double-exponential noise, (f) response of MVD to (e).

distance of \mathbf{X}^i to the set of vectors $\mathbf{X}^1, \mathbf{X}^2, \dots, \mathbf{X}^n$, then

$$d_i = \sum_{k=1}^n \|\mathbf{X}^i - \mathbf{X}^k\| \quad (1)$$

where $\|\cdot\|$ represents an appropriate vector norm. An arrangement of the d_i s in ascending order, $d_{(1)} \leq d_{(2)} \leq \dots \leq d_{(n)}$, associates the same ordering to the multivariate \mathbf{X}^i 's, $\mathbf{X}^{(1)} \leq \mathbf{X}^{(2)} \leq \dots \leq \mathbf{X}^{(n)}$. In the ordered sequence $\mathbf{X}^{(1)}$ is the vector median of the data samples [9]. It is defined as the vector contained in the given set whose distance to all other vectors is a minimum. Moreover, vectors appearing in high ranks in the ordered sequence are vectors that diverge mostly from the data population (outliers).

III. COLOR EDGE DETECTION

In this work, a color image is viewed as a vector field, represented by a discrete vector valued function $\mathbf{f}(\mathbf{x}): Z^2 \rightarrow Z^m$, where Z represents the set of integers.¹ A notation will be used in the following concerning the image function \mathbf{f} . For $W \subset Z^2$, $\mathbf{x}_i \in W$, $i = 1, 2, \dots, n$, n is the size (number of pixels) of W , $\mathbf{f}(\mathbf{x}_i)$ will be denoted as \mathbf{X}^i . $\mathbf{X}^{(i)}$ will denote the i th ordered vector in the window

¹Usually $m = 3$ but the results presented hold for $m \geq 2$.

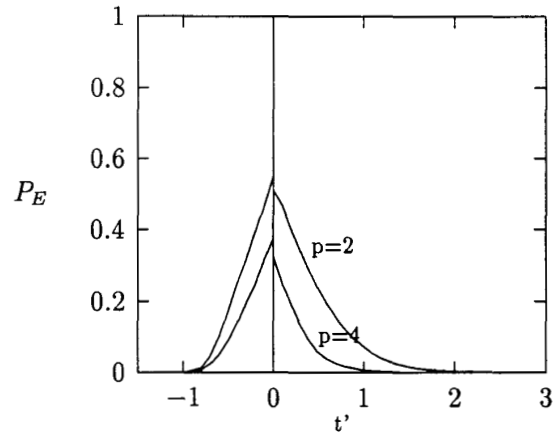


Fig. 2. P_E versus t' (see text for explanation).

W according to the R-ordering method. Consequently, $\mathbf{X}^{(1)}$ is the vector median in the window W and $\mathbf{X}^{(n)}$ is the outlier in the highest rank.

Based on the previous discussion on vector order statistics, a simple color edge detector can be defined as a *vector range*² (VR) edge detector

$$\text{VR} = \|\mathbf{X}^{(n)} - \mathbf{X}^{(1)}\| \quad (2)$$

VR expresses in a quantitative way the deviation of the vector outlier in the highest rank from the vector median in W . Consequently, in a uniform area, where all vectors will be close to each other, the output of VR will be small. However, its response on an edge will be large since $\mathbf{X}^{(n)}$ will be selected among the vectors from the one side of the edge (the smaller side) while $\mathbf{X}^{(1)}$ will be selected among the vectors from the other side of the edge (the larger side). By thresholding the output of VR the actual edges can be obtained. VR would, however, be very sensitive to impulsive type noise since the vectors placed in the higher ranks usually correspond to noisy samples.

This disadvantage leads us to consider dispersion measures which are known as more robust estimates in the presence of noise [10]. A general class of *vector dispersion edge detectors* (VDED) can be defined using linear combinations of the ordered vectors

$$\begin{aligned} \text{VDED} &= \text{OSO} \left(\left\| \sum_{i=1}^n \alpha_{i1} \mathbf{X}^{(i)} \right\|, \left\| \sum_{i=1}^n \alpha_{i2} \mathbf{X}^{(i)} \right\|, \dots, \left\| \sum_{i=1}^n \alpha_{ik} \mathbf{X}^{(i)} \right\| \right) \\ &= \text{OSO}_j \left(\left\| \sum_{i=1}^n \alpha_{ij} \mathbf{X}^{(i)} \right\| \right), \quad j = 1, 2, \dots, k \end{aligned} \quad (3)$$

where OSO denotes an *order statistic operator*. Specific color edge detectors can be obtained from (3) by proper selection of OSO and a set of coefficients α_{ij} . Unfortunately, this task seems to be very difficult to approach in a strict mathematical sense. Consequently, we proceed by placing a number of requirements that an edge detector should fulfill and later we try to satisfy these requirements. The edge detector should at first be insensitive to long-tailed (impulsive or double-exponential) and short-tailed (gaussian) noise. It should also respond properly to ramp edges by giving a higher value (edge strength) to the true edge pixel than the value assigned to the neighboring pixels.

Since impulsive type noise appears in an ordered vector set as noisy samples in the higher ranks, the detector can be made insensitive to

²The name is borrowed from the scalar case where $X^{(n)} - X^{(1)}$ is the range of the ordered random variables.

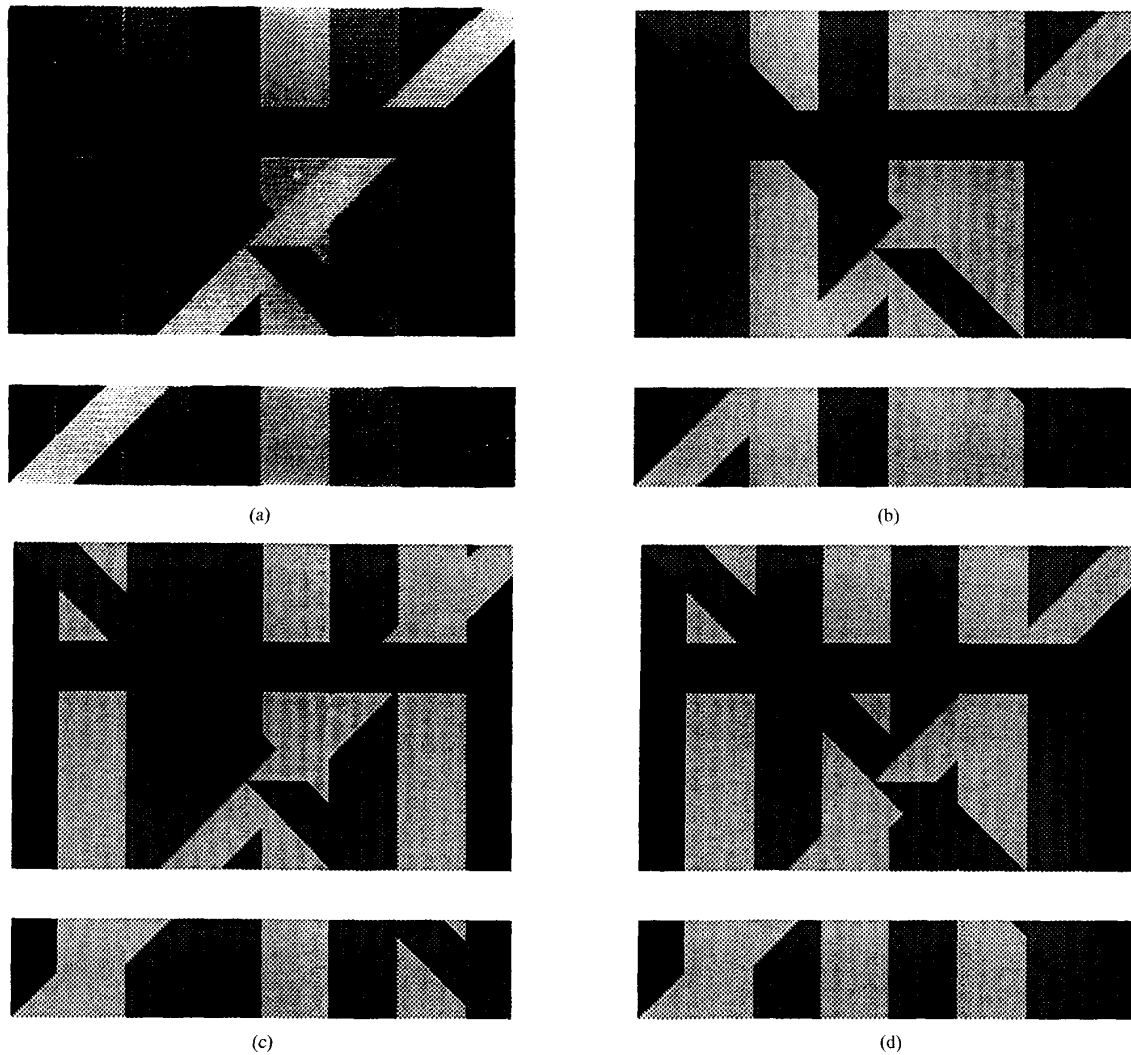


Fig. 3. Artificial image used for testing and comparison purposes (a) image, (b) red component, (c) green component, (d) blue component.

this type of noise by employing k sets of differences instead of the single difference shown in (2) and a minimization operation

$$\min_j \left(\left\| \mathbf{X}^{(n-j+1)} - \mathbf{X}^{(1)} \right\| \right) \quad (4)$$

$j = 1, 2, \dots, k, k < n.$

The effect of the min operator is that fake impulses (up to $k-1$) due to isolated noisy pixels are not detected. Such a minimum operator has also been used in [8] in order to derive an edge detector insensitive to noisy impulses. The choice of k in (4) depends on n , the size of the window W used. For a 3×3 window, for example, $k \leq 3$. Unfortunately, there is no general formula to obtain k and its value should be subjectively estimated. However, this is not a difficult task, since k can be interpreted as the number of pixels that belong to the smaller side of an edge, when W is centered on an edge pixel. Moreover, its value is not crucial in the overall performance of the detector.

For obtaining insensitivity in the presence of short-tailed noise, a better signal estimate than the vector median $\mathbf{X}^{(1)}$ [See (2)] is needed. Consequently, we proceed by replacing $\mathbf{X}^{(1)}$ by the vector α -trimmed

mean ($V_{\alpha}TM$) ($\sum_{i=1}^l (\mathbf{X}^{(i)}/l)$). $V_{\alpha}TM$ has been shown as a robust signal estimate in color images when the noise is modeled as short-tailed [11]. The resulting edge detector, *minimum vector dispersion* (MVD), is given as

$$MVD = \min_j \left(\left\| \mathbf{X}^{(n-j+1)} - \sum_{i=1}^l \frac{\mathbf{X}^{(i)}}{l} \right\| \right) \quad (5)$$

$j = 1, 2, \dots, k, k, l < n.$

The value of the parameter l in (5) cannot be formally defined as it is the case for the parameter k mentioned above. However, a duality exists between these two parameters; l expresses the number of pixels that belong to the larger side of an edge when W is centered on an edge pixel. Therefore, proper values for the parameter l can be subjectively estimated for various sizes of W .

MVD has improved noise performance since the minimum operation makes it insensitive to long-tailed noise and the averaging operation makes it insensitive to short-tailed noise. This is illustrated in Fig. 1. A color edge, plotted as a vector field, is shown in Fig. 1(a) and the response of MVD to this edge is shown in Fig. 1(b). The

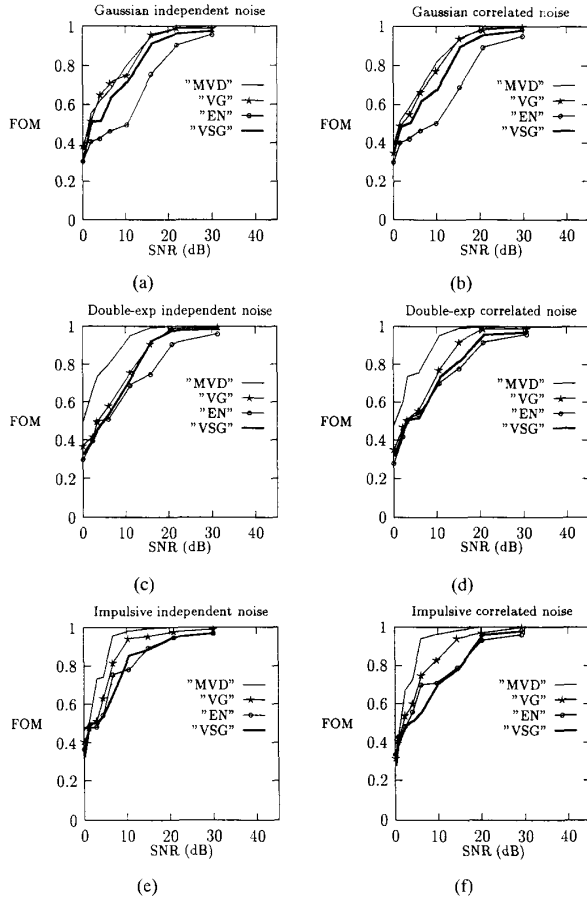


Fig. 4. FOM plots for four color edge detectors: MVD, vector gradient (VG), entropy (EN), vector sum of gradients (VSG).

same color edge is shown in Figs. 1(c), (e) corrupted with gaussian and double-exponential noise, respectively. MVD responds to these two edges as shown in Figs. 1(d), (f). As can be verified, the true edge is given a much larger response and consequently it is easily detected by thresholding. It is also interesting to note that MVD responds to ramp edges by assigning a higher value to the true edge pixel than the values assigned to the neighboring pixels. Thus, for an (1-D) ideal ramp edge of three pixels, the response of MVD will be

$$\begin{array}{c} \diagdown \quad \diagup \quad \diagup \quad \diagdown \\ \cdot \quad | \quad | \quad | \quad \cdot \end{array} \quad \begin{array}{l} \text{(3-pixel ramp edge)} \\ \text{(MVD response)} \end{array}$$

where it is implied that a 3-pixel window is used. For ideal ramp edges of larger size more pixels will be given a high response. However, if the window size is increased the center pixel will again be given a larger response and by proper thresholding it can be detected.

A. Statistical Analysis

The statistical analysis of the proposed color edge detectors is, unfortunately, very difficult. The distribution functions of multivariate order statistics have not been adequately studied in the statistics literature. Most results derived concern multivariate normal distributions and we will consider only these distributions in this section. For our ideal edge model we consider the sample vectors \mathbf{X}_i on the one side of the edge as instances of a random variable \mathbf{X} which follows a

multivariate normal distribution $N_m(\mu_x, I_m)$. Similarly, the sample vectors on the other side of the edge, \mathbf{Y}_i , are instances of the random variable \mathbf{Y} which is $(N_m(\mu_y, I_m))$. Then the error probability is the probability of detecting an edge when no edge is present plus the probability of missing an edge when it is present

$$P_E = P_r\{\min \|\mathbf{Y}_i - \bar{\mathbf{X}}\| > t, \|\mu_y - \mu_x\| \leq t\} + P_r\{\min \|\mathbf{Y}_i - \bar{\mathbf{X}}\| < t, \|\mu_y - \mu_x\| > t\} \quad (6)$$

where $\bar{\mathbf{X}}$ stands for the mean of vectors \mathbf{X}_i . Let the random variable d , with instances d_1, d_2, \dots , denote the distance $\|\mathbf{Y} - \bar{\mathbf{X}}\|$, i.e., $d_i = \|\mathbf{Y}_i - \bar{\mathbf{X}}\|$. Sorting the d_i 's will result in an ordered sequence $d_{(i)}$. Clearly, $d_{(1)} = \min \|\mathbf{Y}_i - \bar{\mathbf{X}}\|$; if we also set $\|\mu_y - \mu_x\| = \tau$ then (6) can be rewritten as

$$\begin{aligned} P_E &= P_r\{d_{(1)} > t, \tau \leq t\} \\ &\quad + P_r\{d_{(1)} < t, \tau > t\} \\ &= P_r\{d_{(1)} - \tau > t', t' \geq 0\} \\ &\quad + P_r\{d_{(1)} - \tau < t', t' < 0\}, \quad t' = t - \tau \\ &= P_r\{d\tau_{(1)} > t', t' \geq 0\} \\ &\quad + P_r\{d\tau_{(1)} < t', t' < 0\} \end{aligned} \quad (7)$$

where $d\tau_{(1)} = d_{(1)} - \tau$. The two terms of (7) can be further rewritten as

$$\begin{aligned} P_r\{d\tau_{(1)} > t', t' \geq 0\} &= P_r\{d\tau_{(1)} > t' | t' \geq 0\} \cdot P_r\{t' \geq 0\} \\ &= [1 - P_r\{d\tau_{(1)} \leq t' | t' \geq 0\}] \cdot P_r\{t' \geq 0\} \\ &= \left[1 - \frac{P_r\{d\tau_{(1)} \leq t', t' \geq 0\}}{P_r\{t' \geq 0\}}\right] \cdot P_r\{t' \geq 0\} \\ &= P_r\{t' \geq 0\} - P_r\{d\tau_{(1)} \leq t', t' \geq 0\} \\ &= P_r\{t' \geq 0\} - \begin{cases} F_{d\tau_{(1)}}(t'), & t' \geq 0 \\ 0 & \text{otherwise} \end{cases} \end{aligned} \quad (8)$$

and

$$P_r\{d\tau_{(1)} < t', t' < 0\} = \begin{cases} F_{d\tau_{(1)}}(t'), & t' < 0 \\ 0 & \text{otherwise} \end{cases} \quad (9)$$

Therefore (7) becomes

$$P_E = P_r\{t' \geq 0\} - F_{d\tau_{(1)}}(t')u(t') + F_{d\tau_{(1)}}(t')u(-t') \quad (10)$$

where $u(x)$ is the unit step function. We note also that $F_{d\tau_{(1)}}(t') = F_{d_{(1)}}(t)$ since

$$F_{d\tau_{(1)}}(t') = P_r\{d\tau_{(1)} \leq t'\} = P_r\{d_{(1)} \leq t\}$$

and $F_{d_{(1)}}$ can be obtained from F_d , the distribution function of d as [10, p. 8]:

$$F_{d_{(1)}}(x) = 1 - [1 - F_d(x)]^p \quad (11)$$

where p denotes the number of sample distances. In our case $p = k$ [see (5)]. The problem is now reduced to the estimation of F_d . If we consider Euclidean distances, then $d^2 = \|\mathbf{Y} - \bar{\mathbf{X}}\|^2 = (\mathbf{Y} - \bar{\mathbf{X}})^T (\mathbf{Y} - \bar{\mathbf{X}})$ which follows a noncentral chi-square distribution with m degrees of freedom and noncentrality parameter $s = (\mu_y - \mu_x)^T (\mu_y - \mu_x)$ [12, p. 19]. There is no closed form expression of the cumulative distribution function of the noncentral chi-square distribution. For the case, however, where $z = m/2$ is an integer it can be expressed in terms of the generalized Q function [13]

$$F_{d^2}(y) = 1 - Q_z(s, \sqrt{y}). \quad (12)$$



Fig. 5. Edge detection results. (a) Original image, (b) MVD, (c) vector gradient, (d) entropy, (e) vector sum of gradients.

Since the distances d are nonnegative, F_d can be obtained from (12) by a simple change in variables

$$\begin{aligned} F_d(y) &= P_r\{d \leq y\} = P_r\{d^2 \leq y^2\} \\ &= F_{d^2}(y^2) = 1 - Q_z(s, y). \end{aligned} \quad (13)$$

From (13), (11) can be computed and (10) can also be computed provided that $P_r\{t' > 0\}$ is known. For our model, $t' = t - \tau$, where t is the detector's threshold (deterministic quantity) and $\tau = \|\mu_y - \mu_x\|$ (constant). Therefore, t' is a deterministic quantity and $P_r\{t' \geq 0\}$ is unit or zero for $t' \geq 0$ or $t' < 0$, respectively.

P_E is shown in Fig. 2 for $m = 2$ and two p values, $p = 2$ and $p = 4$. In the computation of P_E , a value of $\tau = 1$ (edge height) has been used which is in accordance with the noise level assumed (unit covariance matrix- I_m). From (10), (11) and Fig. 2 we can conclude that the probability of error P_E is decreased with respect to p . Since p increases with the window size n , P_E decreases with respect to n . However, there is a tradeoff since a large window has a negative effect in accurate edge localization and, therefore, large n values should be avoided.

IV. EXPERIMENTAL RESULTS

The proposed color edge detector has been evaluated both quantitatively and qualitatively. For quantitative evaluation and comparison to other color edge detectors, Pratt's figure of merit (FOM) [14] has been used as a performance measure. FOM is defined as

$$\text{FOM} = \frac{1}{\max\{I_D, I_I\}} \sum_{i=1}^{I_D} \frac{1}{1 + \alpha(d_i)^2} \quad (14)$$

where I_D, I_I are the number of detected and number of ideal edge points respectively, $\alpha(>0)$ is a calibration constant, and d_i is the edge deviation for the i th detected edge pixel. In all cases $0 < \text{FOM} \leq 1$; for a perfect match between the detected and the ideal edges FOM = 1 whereas the detected edges deviate more and more from the ideal ones FOM goes to zero. The scaling constant $\alpha = 1/9$ proposed in [14] has been adopted.

An artificial image has been created and used as a benchmark for assessing the performance of MVD and for comparison purposes. It is shown in Fig. 3 along with its R, G, B components. A number of edge detection experiments have been conducted using various types of noise and various noise levels to contaminate this test image. In each case, FOM has been measured and used as the performance criterion. The noise types used were gaussian, double-exponential and impulsive. For each noise type two sets of experiments have been performed. In the first set, the noise process in each channel has been considered as an independent process. In the second set, the noise process has been considered as a correlated process (a correlation factor 0.5 has been used) since there is some indication that this type of correlation may exist in real color images. For comparison purposes, three other color edge detectors have been applied on the same image: The vector gradient operator [4]; the entropy operator [3]; and the vector sum of the gradients of the three color components. The last operator has been selected among the operators that result from combining componentwise edge detectors since it produces results that are generally better [15].

The performance measures obtained are shown in Fig. 4. As can be verified, all the operators have good performance for low noise levels, although the performance of MVD is slightly better. However, as the SNR decreases, the superiority of the proposed MVD becomes clear for all the noise types. The performance of the vector gradient operator is close enough to the performance of MVD for gaussian noise but is inferior for double-exponential and impulsive noise.

The other two operators have lower performance measures. The performance of the entropy operator is largely degraded as noise increases.

In all the experiments described above, the values used for the parameters of the MVD operator were as follows: 5×5 window, $k = 8, l = 12$. It should be noted here that the selected values of k and l have been experimentally obtained and, more importantly, they are not critical in the overall performance. Practically, the performance has been left unchanged for $7 \leq k \leq 10$ and $10 \leq l \leq 15$. Regarding the window size it is noted that even a 3×3 window has given very good results when the noise level is low. However, for higher noise levels the 5×5 window results in better performance since it involves more pixels in the edge detection process.

Subjectively, the performance of MVD has been assessed using real color images. Experiments using many different kinds of images have been conducted; the edge detection results for a girl's face are presented here. The original image is shown in Fig. 5(a) whereas the edge detection results are presented in Fig. 5(b). The results of the color edge detectors used for comparison are also shown in Figs. 5(c), (d), and (e), respectively. A visual evaluation gives the impression that the MVD and the vector gradient perform comparably. However, MVD appears less sensitive to small texture variations (see the cheek and the shoulder for example). This can be ascribed to the averaging operation which essentially smooths out small variations whereas the gradient-based operators are sensitive even to small changes. The entropy operator is totally insensitive to texture variations but on the other hand it leaves undetected many edges that correspond to fine image details (see the shoulder line or the lips, for example). The vector sum of the gradients operator, although sensitive to the image details, is faced with the problem that it cannot detect some very simple edges (see the frame, for example) when the gradients of the image components change in the opposite direction.

REFERENCES

- [1] R. Nevatia, "A color edge detector and its use in scene segmentation," *IEEE Trans. Syst. Man, Cybern.*, vol. SMC-7, pp. 820-825, Nov. 1977.
- [2] G. Robinson, "Color edge detection," *Opt. Eng.*, vol. 16, pp. 479-484, 1977.
- [3] A. Shiozaki, "Edge extraction using entropy operator," *Computer Vision Graphics and Image Proc.*, vol. 36, pp. 1-9, 1986.
- [4] S. Zeno, "A note on the gradient of a multiimage," *Computer Vision Graphics and Image Proc.*, vol. 33, pp. 116-125, 1986.
- [5] A. Cumani, "Edge detection in multispectral images," *CVGIP: Graphical Models and Image Proc.*, vol. 53, pp. 40-51, Jan. 1991.
- [6] R. Machuca and K. Phillips, "Applications of vector fields to image processing," *IEEE Trans. Patt. Anal. Mach. Intell.*, vol. PAMI-5, pp. 316-329, May 1983.
- [7] V. Barnett, "The ordering of multivariate data," *J. Royal Statistical Society A*, vol. 139, Part 3, pp. 318-343, 1976.
- [8] J. Lee, R. Haralick, and L. Shapiro, "Morphologic edge detection," *IEEE J. Rob. and Autom.*, vol. RA-3, pp. 142-156, Apr. 1987.
- [9] J. Astola, P. Haavisto, and Y. Neuvo, "Vector median filters," *Proc. IEEE*, vol. 78, pp. 678-689, Apr. 1990.
- [10] H. David, *Order Statistics*. New York: Wiley, 1980.
- [11] S. Sanwalka and A. Venetsanopoulos, "Vector order statistics filtering of colour images," in *Thirteenth GRETSI Symp. on Signal and Image Proc.*, pp. 785-788, 1991.
- [12] G. Seber, *Multivariate Observations*. New York: Wiley, 1984.
- [13] J. Proakis, *Digital Communications*. New York: McGraw-Hill, 1989.
- [14] I. Abdou and W. Pratt, "Quantitative design and evaluation of enhancement/thresholding edge detectors," *Proc. IEEE*, vol. 67, pp. 753-763, 1979.
- [15] W. Pratt, *Digital Image Processing*. New York: Wiley, 1991.